[Review] DOI: 10.13208/j.electrochem.2213002 Http://electrochem.xmu.edu.cn

Research Progress in Electroless Cobalt Plating and the Bottom-up Filling of Electroless Plating

Yu Shen, Bing-Bing Li, Yi Ma, Zeng-Lin Wang*
(*Shaanxi Normal University, School of Chemistry and Chemical Engineering, Xi'an 710062, Shaanxi, China*)

Abstract: With the continuous improvement of semiconductor integration, the resistivity of copper interconnect lines increases rapidly. When the width of the interconnect line is close to 7 nm, the resistivity of copper becomes the same as that of cobalt. International Business Machines Corporation (IBM) and Advanced Semiconductor Incorporation (ASI) have used cobalt to replace copper as a next-generation interconnect material. However, the fabrication of the cobalt seed layer and the super filling of electroplating cobalt for the 7 nm via-holes have been still the large challenge. Electroless plating is a very simple method to form a seed layer on the surface of an insulator. By the bottom-up filling of electroless plating, via-holes with several nanometers could be filled completely. In this paper, the research progress in electroless cobalt plating is reviewed, and the effects of the reductant species on the deposition rate and the film quality of electroless cobalt plating are analyzed. Meanwhile, based on long-term and a lot of studies, a bottom-up filling of electroless cobalt plating for 7 nm via-hole in semiconductor cobalt interconnects is proposed.

Key words: electroless cobalt plating; bottom-up filing; electroless copper plating; super electroless cobalt plating; copper interconnects; cobalt interconnects

1 Introduction

The continuous miniaturization of electronic products has led to a further increase in wiring density and metal layer stacking, and a dramatic reduction in the size of metal interconnect features. Decreasing dimensions also lead to greater RC delay and IR drop due to the exponential increase in resistivity with decreasing line cross-section. When the IC industry moves beyond the 10 nm node, the electrical resistivity of copper interconnects rapidly rises at the critical dimension of the back-end-of-line (BEOL) due to increasing electron scattering from small copper particles and diffusing surfaces[1].

The main factor that affects the resistivity of metal thin films is grain boundary scattering. Because of a short electron mean free path (MFP), the resistivity of metal cobalt is less affected by the grain. When the width of interconnect line reaches 7 nm, the thin-film resistivity of cobalt metal is similar to that of copper metal, and so metal cobalt is considered to be the next-generation interconnect metal[2]. Figure 1 shows via resistance measurements for cobalt and copper filled vias in contact with the underlying copper layer. Although cobalt has three times the resistivity of copper, the difference in via resistance between cobalt and copper is very small[3]. Meanwhile, the copper interconnect requires a TaN barrier layer with a thickness of about 2 nm to prevent metal from diffusing into the Si/SiO_2 layer, which also reduces the effective filling volume of the interconnection, and results in a further increase in interconnection resistance[4]. Cobalt interconnect can be deposited directly on dense low-K dielectrics with C content of 24% or above without electron drift and does not require an

Cite as: Shen Y, Li B B, Ma Y, Wang Z L. Research progress of electroless cobalt plating and the bottom-up filling of electroless plating. *J. Electrochem.*, 2022, 28(7): 2213002.

Received: 2022-04-02, Revised: 2022-05-07. *Corresponding author, Tel: (86-29)81530761, E-mail: wangzl@snnu.edu.cn

anti-diffusion layer to prevent metal electrons from diffusing into the dielectric film[5]. The thermal expansion coefficient of cobalt is close to that of silicon, which makes cobalt become a compatible metal for integration in silicon-based electronic chips. Until now, cobalt interconnect line has been recommended as the next-generation interconnect metal to meet the needs of current and next-generation communication equipment by Intel and Advanced Semiconductor. Cobalt metal also acts as a barrier layer or an adhesion layer, which is beneficial to increase the volume ratio of metal conductors in nano-holes or vias and to further improve the electrical conductivity of interconnect lines.

And now, cobalt interconnects in IC have been fabricated by bottom-up electroplating cobalt filling. However, there are only a few reports about electrodepositing cobalt filling nano-holes or vias in chip[6, 7]. Due to the negative reduction potential of Co^{2+}, the hydrogen evolution occurs in the electroplating process, and the surface uniformity of deposited cobalt film also is a challenge[8]. The electroless plating does not need a seed layer, and its process is simple and low cost. In addition, our group has been engaged in the research of electroless copper for a long time, and has realized the bottom-up electroless copper and nickel filing for sub-micro via-holes. Therefore, based on the present research of electroless cobalt plating,

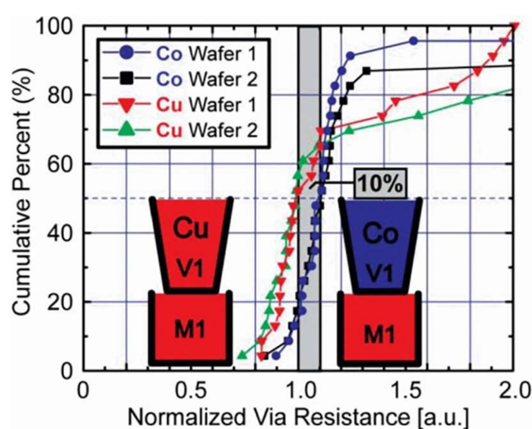

Figure 1 Cumulative percent of normalized resistance for the via filled by Cu or Co (Reproduced with permission of Ref. 3, Copyright 2011 IEEE)

we propose a new research plan, i.e., bottom-up electroless cobalt to fill via of 7 nm or less chip for cobalt interconnects.

2 Electroless Cobalt Plating

The electroless plating of cobalt has been first reported by Brenner and Riddle[9] and used to deposit metal cobalt on the plastics. Because of the unique strong magnetic properties of the deposited cobalt, electroless cobalt plating had been studied widely. Meanwhile, the magnetic properties of cobalt film could be adjusted by the bath composition and the operation parameters. In addition, electroless cobalt films and alloys could be used as barrier layers in Damascus copper interconnects process.

2.1 Electroless Co-P Plating Using Sodium Hypophosphite as a Reductant

Electroless Co-P plating using sodium hypophosphite (NaH_2PO_2) as a reducing agent has been studied widely and the magnetic properties of the film could be adjusted by the P content in the film. When the content of P is more than 5 wt%, the Co-P deposited film becomes an amorphous. Though the co-deposition of Co-P is benefitted to the improvement of wear resistance, the electrical conductivity of cobalt film also increased with the P content.

The electroless Co-P plating solution uses cobalt sulfate as the cobalt source, sodium citrate and sodium tartrate as complexing agents, and the pH of the solution may be controlled to be about 8-11. Frieze, et al.[10-12] found that the deposited particle size and density of Co-P film depended strongly on NaH_2PO_2 concentration and the bath temperature. Liu et al. deposited the electroless Co-P films on Si wafers[13]. Yu et al.[14] investigated the effects of the ultrasonic wave on the deposition rate of electroless Co-P plating and surface morphology. The deposition rate could be enhanced clearly by the ultrasonic wave treatment due to the quickly escape of H_2 bubbles generated in the electroless plating and temperature increase of the bath. In addition, the high-power ultrasound caused a high molecular collision on the surface of the film, resulting in a smooth Co-P coating (Figure 2). Magagnin et al.[15] reported that the high pH in the bath was

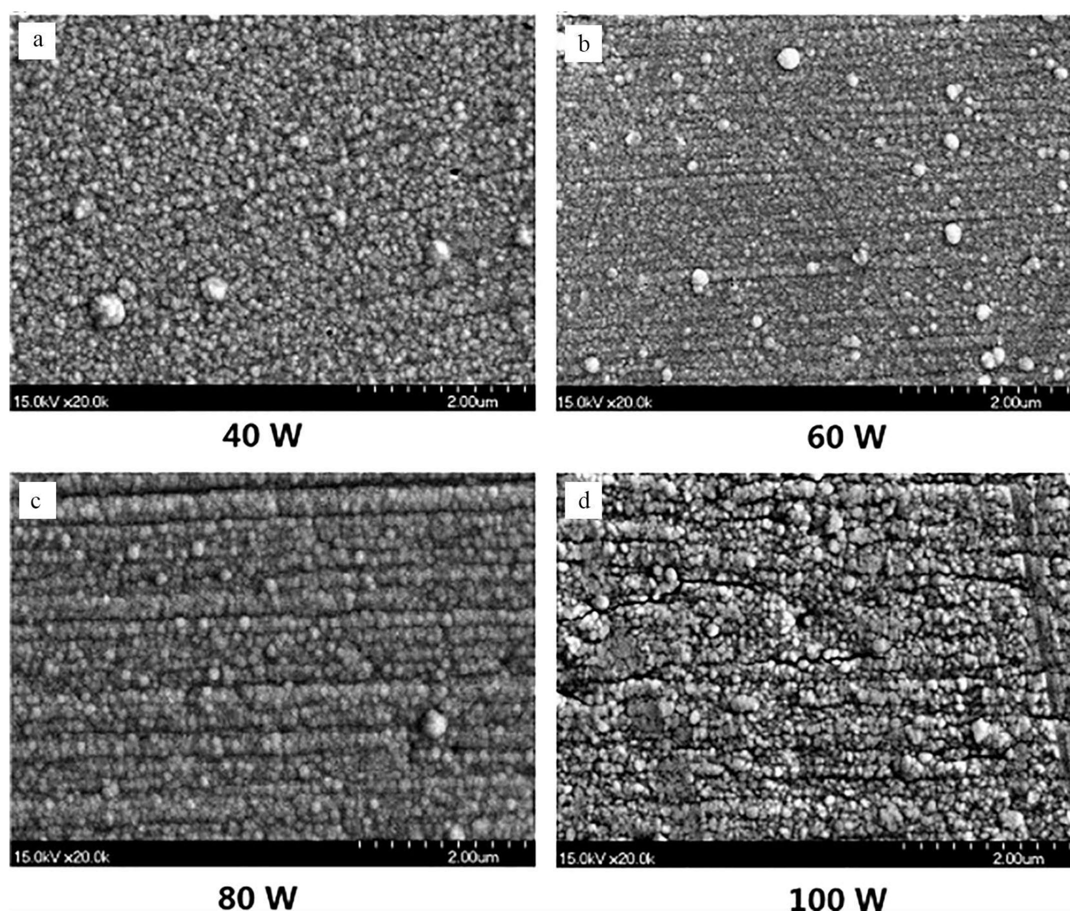

Figure 2 The effects of ultrasonic powers on surface morphology of Co-P films (Reproduced with permission of Ref. 14, Copyright 2014 Chinese MRS)

beneficial to the increase of the deposition rate and had a little effect on the P content in the coating.

2.2 Electroless Co-B Plating System Using Boride as a Reductant

2.2.1 Sodium Borohydride ($NaBH_4$) as a Reductant

Co-B films have higher hardness, corrosion resistance, and melting point than those of Co-P films. When $NaBH_4$ is used as a reductant in the cobalt plating solution, the $NaBH_4$ concentration affects directly the deposition rate and stability of the solution. With the increase of the reductant concentration, the electroless cobalt deposition rate can be enhanced markedly, but the stability of the bath decreased. Due to the high boron content in the coating, the resistivity of electroless Co-B film can be much higher than that of pure cobalt film.

Chang et al. [16] deposited successfully the amorphous Co-B binary alloy on copper sheet in the electroless cobalt solution by using $NaBH_4$ as a reducing agent, and after annealing at 220 ℃ in He/H_2 atmosphere, the amorphous Co-B alloy was transformed into a hexagonal close-packed cobalt. Deng group [17] investigated the formula of Co-B electroless plating solution by an orthogonal experiment. After an annealing treatment, the amorphous CoB alloy was changed to Co_2B crystalline[18].

2.2.2 Dimethylamine Borane (DMAB) as a Reductant

When dimethylamine borane (DMAB) is used as a reductant and the bath temperature is controlled at 75 ℃, the electroless cobalt plating solution exhibits a wide pH operating range and strong regeneration ability. It has been reported that DMBA has a low redox potential and is able to reduce Co^{2+} to metal cobalt in acidic or alkaline baths[19], but the oxidation

rate of DMAB is very slow in the absence of Pd activation.

The reducing ability of DMAB is between sodium borohydride ($NaBH_4$) and sodium hypophosphite (NaH_2PO_2), and the stability of the plating solution is better than that of $NaBH_4$ solution. The bath stability and the boron content in the CoB coating were found to be affected by the bath pH, and the boron content in the coating was decreased with the increase of the pH vale[20].

Saito et al.[21] found that the boron content in CoB film was influenced by the coordination ability of complexing agent. For complexing agent with strong coordination ability, the deposition rate of the bath was reduced and the boron content in the coating was increased, resulting into a formation of amorphous Co-B films. Shacham-Diamand et al. [22] studied the effects of DMAB concentration on the deposition rate, resistance, element distribution and surface roughness in the films, and found that the boron content in the film was determined by the surface adsorption rate of the reductant. Stankeviciene et al. [23] found that the induction period and the deposition rate of the electroless cobalt solution could be shortened and enhanced with an addition of diethylenetriamine. Ivan et al. [24] found that the deposited amorphous Co-B films could be transformed into hexagonal close-packed cobalt in H_2/N_2 atmosphere with an increase of annealing temperature (Figure 3). Chang et al.[25] deposited electroless Co on the surface of copper wires by a selective autocatalytic process and the sheet resistance (R_s) of the deposited film with a boron content of 1.4 at.% ~ 4.4 at.% was lower than that of the Pd-catalyzed cobalt film.

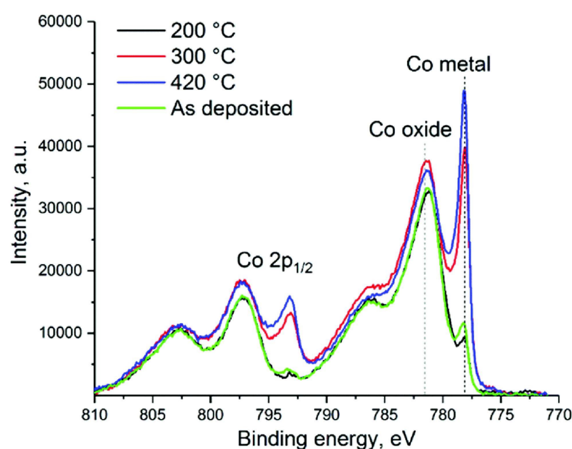

Figure 3 Co 2p high-resolution XPS spectra of Co-B film after annealing treatment in H_2/N_2 atmosphere with various temperatures (Reproduced with permission of Ref. 24, Copyright RSC 2019).

2.3 Electroless Co Plating Using Hydrazine (N_2H_4) as a Reductant

Electroless Co plating using NaH_2PO_2, $NaBH_4$ and DMAB as reductants is easy to incorporate a certain amount of P and B in the cobalt film, which affects the conductivity, crystallinity and solderability. However, when hydrazine is used as a reductant, almost pure metal Co film may be obtained.

The composition of electroless cobalt plating with hydrazine as a reductant is as follows: cobalt sulfate or cobalt chloride as a cobalt source, and sodium citrate or sodium tartrate as a complexing agent. Cheng et al.[26] obtained a pure metallic cobalt film with hexagonal close-packed crystal structure in electroless cobalt solution. Yagi et al.[27] found that H_2PtCl_6 addition could provide nucleation sites for cobalt deposition, and the particle size and its distribution became clear. Stojan et al.[28] reported that the deposition rate was increased with the increases of pH, bath temperature and concentrations of hydrazine and Co^{2+}, but the surface roughness of the electroless cobalt film was increased correspondingly with the above-mentioned factors (Figure 4). Ohno et al.[29] investigated the anodic oxidation catalytic activity of different reductants and found that the anodic oxidation potential for hydrazine (-0.940 V) in electroless cobalt plating solution was lower than these for DMAB (-0.832 V) and NaH_2PO_2 (-0.854 V), which indicated that hydrazine has a stronger reducing ability than DMAB or NaH_2PO_2.

Although hydrazine can be used as a reductant to obtain a high-purity cobalt film, H_2 and N_2 are easily incorporated to the film, causing hydrogen embrittlement. The doped gas could be escaped by heat treatment, and the stress and electrical resistivity of the electroless cobalt film could be guaranteed. However,

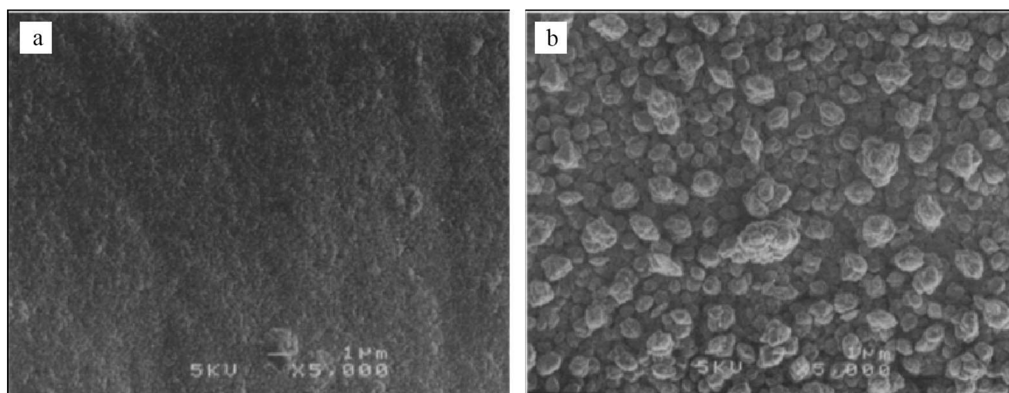

Figure 4 SEM images of electroless Co films, bath components: $C_{N_2H_4}$ = 0.032 mol·L^{-1}, $C_{Co^{2+}}$ = 0.08 mol·L^{-1}, deposition condition: (a) pH = 12.13, T = 62.5 °C; (b) pH= 12.73, T = 72 °C (Reproduced with permission of Ref. 28, Copyright 1997 The Electrochemical Society).

the biggest problem for hydrazine system is the very low deposition rate, less than 1 μm·h^{-1}.

3 Bottom-up Electroless Filling for Sub-Micro Via-Holes in Semiconductor Interconnection Line

3.1 Bottom-up Electroless Copper Filling Solution

3.1.1 Single Additive for Bottom-up Electroless Copper Filling

Although sodium polydithiodipropyl sulfonate (SPS) has been also widely used in the field of electroplating copper filling technology[30,31], Shingubara and Wang et al.[32-35] first realized the bottom-up electroless copper filling of sub-micron via-holes using SPS as an accelerator and glyoxylic acid as a reducing agent (Figure 5). It was found that the diffusion coefficient of additives played a crucial role in realizing bottom-up electroless copper plating. Kim et al.[36] also achieved bottom-up electroless copper plating filling of micro-holes with an appropriate addition of SPS in formaldehyde electroless copper solution. Osaka et al.[37] found that polyethylene glycol (PEG) with a molecular weight of 4000 (PEG-4000) could reduce the deposition rate of electroless copper plating using glyoxylic acid as a reducing agent. Due to the large molecular weight and slow diffusion rate of PEG-4000, a concentration gradient of PEG in the via-holes was formed, which resulted in that the deposition rate of electroless copper in the bottom of the sub-micro hole is much higher than that on the surface (Figure 6a), and a perfect bottom-up electroless copper plating filling was achieved (Figure 6b). Wang et al.[38] compared bottom-up filling in electroless plating with the additions of PEG, PPG and EPE, and found that a perfect filling of electroless copper could be achieve by an addition of EPE-2000 (Figure 7a)

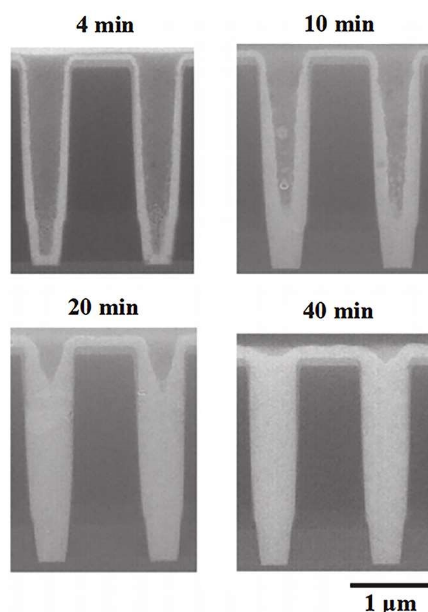

Figure 5 Cross-sectional SEM images of electroless copper filled trenches for different time in the solution containing 0.5 mg·L^{-1} SPS (Reproduced with permission of Ref. 34, Copyright 2004 The Electrochemical Society).

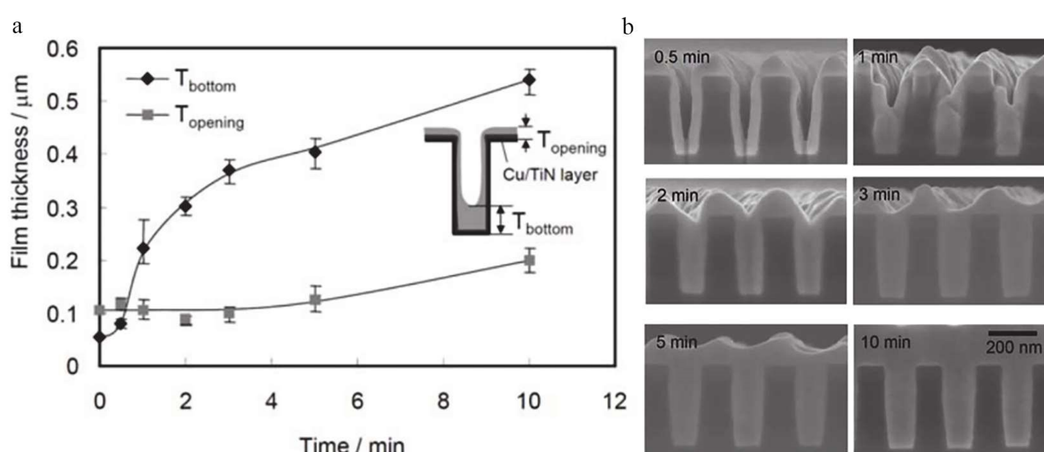

Figure 6 (a) Variations of the thickness of copper deposit with time at the bottom (T_{bottom}) and at the opening ($T_{opening}$) of trenches; (b) Cross-sectional SEM images of electroless copper filled trenches for different time in the solution containing 1 mg·L^{-1} PEG-4000 (Reproduced with permission of Ref. 37, Copyright 2007 American Institute of Physics).

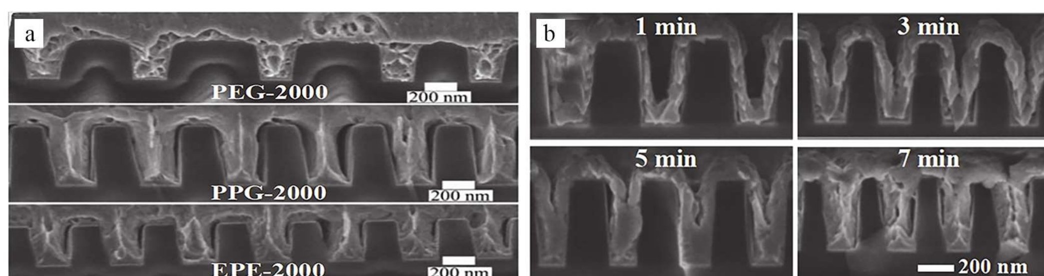

Figure 7 (a) Cross-sectional SEM images of electroless Cu filled profiles with additions of 2.0 mg·L^{-1} PEG-2000 (top), PPG-2000 (middle) and EPE-2000 (bottom); (b) Cross-sectional SEM images of electroless copper filled trenches with different deposition time in the solution containing 1 mg·L^{-1} EPE-8000 (Reproduced with permission of Ref. 39, Copyright 2010 The Electrochemical Society).

due to the strongest inhibition among the three additives. Further, the effects of additives triblock copolymer PEP-3100 and EPE-8000 on bottom-up filling in electroless copper plating were also investigated[39, 40]. Figure 7b shows the cross-sectional SEM images of electroless copper filled trenches with different deposition time in the solution containing 1 mg·L^{-1} EPE-8000.

3.1.2 Formation of the Bottom-up Electroless Copper Filling with the Synergistic of Accelerator and Inhibitor

In order to achieve complete bottom-up filling of electroless plating, the deposition rate of electroless copper in the bottom should be much higher than that on the surface of substrate. And so, a synergistic effect between the accelerator and inhibitor is designed. When the accelerator with a small molecular weight (MW) and the inhibitor with a large MW are added into the electroless copper solution, the distribution of accelerator in the via-hole is uniform, but the inhibitor adsorbs much more on the surface than that in the bottom of via-holes, and a concentration gradient of the inhibitor in the hole is formed. Through the synergistic action of the inhibitor and accelerator, the deposition was accelerated in the bottom of holes and was suppressed on the surface of the substrate, and a perfect bottom-up electroless copper filling without voids and gaps were achieved. Osaka et al.[41, 42] found that when 8-hydroxy-7-iodo-5-quino line sulfate (HIQSA) and PEG-4000 were added to the electroless copper

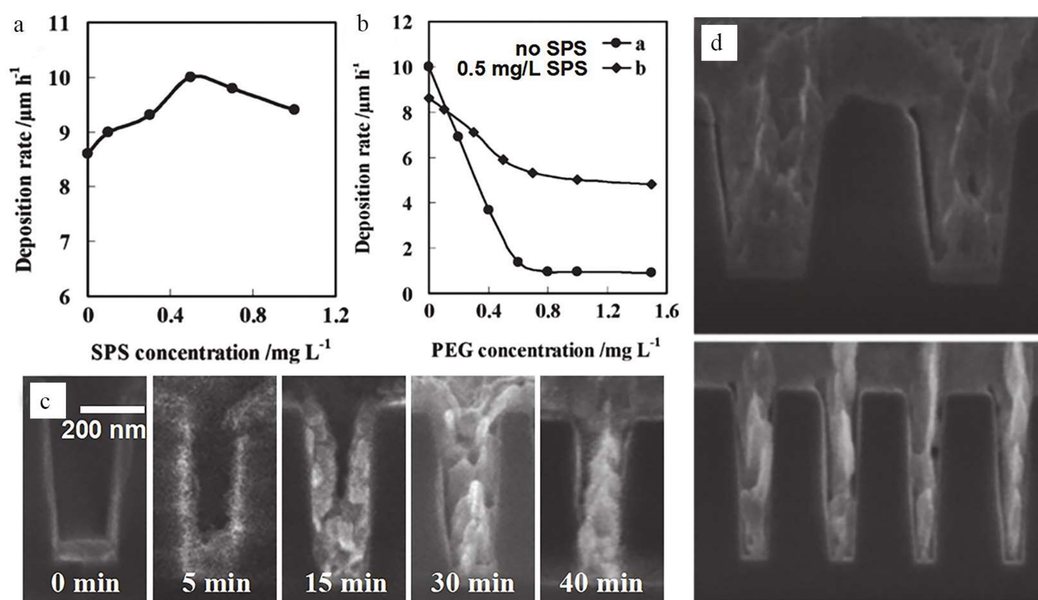

Figure 8 (a) Effect of SPS concentration on the deposition rate of electroless Cu; (b) Effect of PEG concentration on the deposition rate of electroless Cu; Cross-sectional SEM images of electroless Cu filled trenches for different deposition time (c) and with different sizes (d) in the solution containing 1 mg·L^{-1} PEG-4000 and 0.5 mg·L^{-1} SPS (Reproduced with permission of Ref. 44, Copyright 2011 Elsevier Ltd.).

plating solution using formaldehyde as a reductant, the electroless copper deposition was accelerated by HIQSA in the bottom of the micro-holes and was inhibited by PEG-4000 at the top of the holes. Wang et al.[43, 44] found that there existed a synergistic effect between SPS and PEG-4000 in the electroless copper plating solution using formaldehyde or glyoxylic acid as a reductant. The copper deposition was inhibited by the high concentration PEG on the surface of the via-hole and was accelerated simultaneously by the low concentration PEG in the bottom of the via-hole (Figure 8a and 8b), and the micro-trenches with a width of 100 ~ 290 nm were filled by the electroless copper (Figure 8c and 8d). When 2-mercaptobenzothiazole as an accelerator and polyether with an average MW of 3650 as an inhibitor were added in the electroless copper plating solution, the bottom-up electroless copper plating filling was also achieved[45].

3.2 Bottom-up Electroless Nickel Plating

Wang et al.[46] first reported bottom-up electroless nickel plating to fill micro-holes. Polyacrylic acid (PAA) with a MW of 3000-5000 could effectively inhibit the deposition rate of nickel in bath (Figure 9a). When the PAA concentration was 2.0 mg·L^{-1}, the deposition rate of electroless nickel was reduced to 36% of the bath without PAA. Therefore, a perfect bottom-up electroless nickel filling of sub-micro-holes with widths from 80 to 260 nm was obtained in electroless nickel plating bath with an addition of 2.0 mg·L^{-1} PAA (Figure 9b and 9d).

3.3 Bottom-up Electroless Cobalt Plating

Though IBM and ASE companies have replaced some copper interconnects with cobalt interconnects in 7 nm interconnection by bottom-up cobalt electroplating filling, the fabrication of the cobalt seed layer and the bottom-up electroplating cobalt filling are still the large challenge. The electroless plating does not require any seed layer, and the electroless copper and nickel depositions are able to fill sub-microholes. It is, therefore, very necessary to research and develop bottom-up filling of electroless cobalt plating for the 7 nm interconnection line.

4 Summary and Outlook

In this paper, the research progress of the electroless cobalt deposition is reviewed, and the effects of the reductant kinds and plating conditions on the

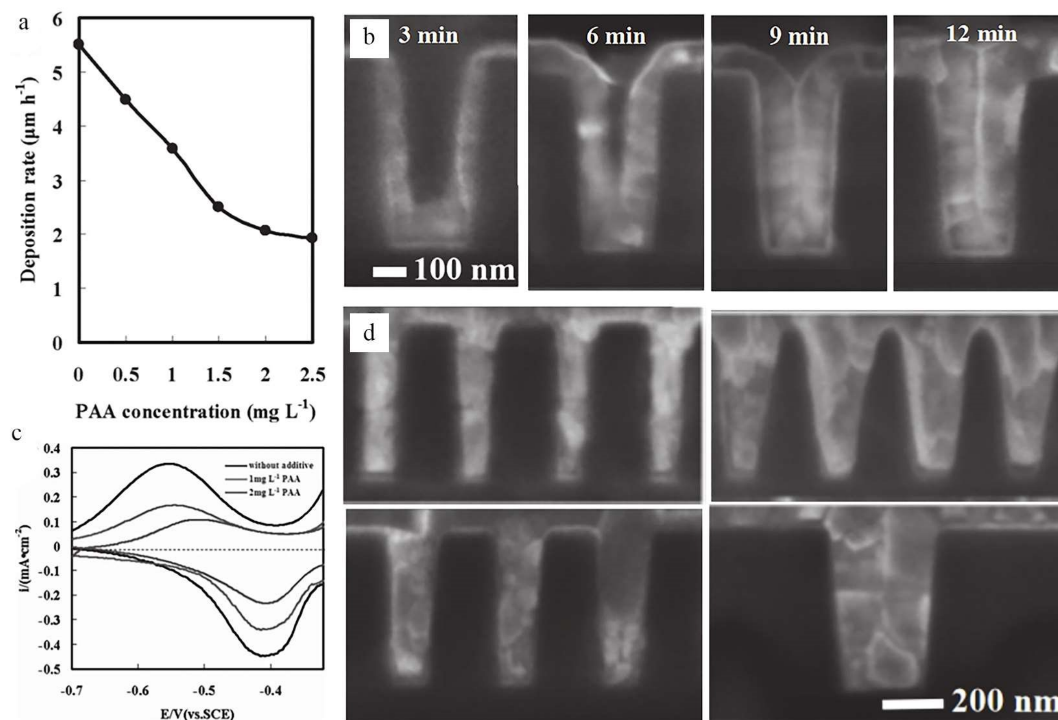

Figure 9 (a) Effect of PAA mass concentration on the rate of electroless Ni deposition; (b) Cross-sectional SEM images of electroless Ni filled trenches for different time in the solution containing 2 mg·L^{-1} PAA; (c) Effect of PAA on the polarization behavior of electroless Ni plating bath; (d) Cross-sectional SEM images of electroless Ni filled trenches with different sizes (Reproduced with permission of Ref. 44, Copyright 2012 The Electrochemical Society).

quality of the cobalt film are discussed. When hydrazine is used as a reductant, a pure cobalt deposition film may be obtained, but the deposition rate of the solution is very low. On the other hand, the researches of the bottom-up filling submicro via-holes by electroless copper plating or electroless nickel plating are summarized. The bottom-up filling mechanisms for electroless plating by an inhibitor and/or synergy effects of inhibition and accelerate are discussed. On the basis of the research development and realistic industrial demand, a bottom-up filling of electroless cobalt for 7 nm via-hole in semiconductor cobalt interconnects is proposed.

Acknowledgements:

The project was financially supported by the National Natural Science Foundation of China (No. 21972088).

References:

[1] Beyne S, Dutta S, Pedreira O V, Bosman N, Adelmann C, De Wolf I, Tokei Z, Croes K. The first observation of p-type electromigration failure in full ruthenium interconnects [C]. Beyne S, IEEE International Reliability Physics Symposium, USA: IEEE, 2018.

[2] Sondheimer E H. The mean free path of electrons in metals[J]. Adv. Phys., 2001, 50(6): 499-537.

[3] Mont F W, Zhang X Y, Wang W, Kelly J J, Standaert T E, Quon R, Ryan E T. Cobalt interconnect on same copper barrier process integration at the 7 nm node[C]. Mont F W, 2017 IEEE International Interconnect Technology Conference (IITC), USA: IEEE, 2017.

[4] Wen D W, Kuwahara H, Kato H, Kobayashi M, Sato Y, Masaki T, Kakihana M. Anomalous orange light-emitting $(Sr,Ba)_2SiO_4$: Eu^{2+} phosphors for warm white LEDs[J]. ACS Appl. Mater. Interfaces, 2016, 8(18): 11615-11620.

[5] Webb E, Witt C, Andryuschenko T, Reid J. Integration of thin electroless copper films in copper interconnect metallization[J]. J. Appl. Electrochem., 2004, 34(3): 291-300.

[6] Ni X R, Chen Y M, Jin X F, Wang C, Huang Y Z, Hong Y, Su X H, Zhou G Y, Wang S X, He W, Chen Q G. Investigation of polyvinylpyrrolidone as an inhibitor for trench super-filling of cobalt electrodeposition[J]. J. Taiwan Inst. Chem. Eng., 2020, 112: 232-239.

[7] Buckalew B, Oberst J, Ponnuswamy T. Electrodeposited cobalt for advanced packaging applications[C]. Buckalew, 2017 IEEE Electron Devices Technology and Manufacturing Conference (EDTM), USA: IEEE, 2017.

[8] Kongstein O E, Haarberg G M, Thonstad J. Current efficiency and kinetics of cobalt electrodeposition in acid chloride solutions. Part I: The influence of current density, pH and temperature[J]. J. Appl. Electrochem., 2007, 37(6): 669-674.

[9] Pearlstein F, Weightman R F. Electroless cobalt deposition from acid baths[J]. J. Electrochem. Soc., 1974, 121: 1023-1023.

[10] Frieze A S, Sard R, Weil R. Some properties of electroless cobalt[J]. J. Electrochem. Soc., 1968, 115: 586-586.

[11] Khan M R, Lee J I. Comparison of plated Co-P and sputtered Co-Re as recording media based on nucleation, growth, structure, and magnetics[J]. J. Appl. Phys., 1985, 57(8): 4028-4030.

[12] Hwang B J, Lin S H. Reaction mechanism of electroless deposition: Observations of morphology evolution during nucleation and growth via tapping mode AFM[J]. J. Electrochem. Soc., 1995, 142(11): 3749-3754.

[13] Liu W L, Hsieh S H, Tsai T K, Chen W J. Growth kinetics of electroless cobalt deposition by TEM[J]. J. Electrochem. Soc., 2004, 151(10): C680-C683.

[14] Yu Y D, Song Z L, Ge H L, Wei G Y. Preparation of CoP films by ultrasonic electroless deposition at low initial temperature[J]. Prog. Nat. Sci., 2014, 24(3): 232-238.

[15] Magagnin L, Sirtori V, Seregni S, Origo A, Gavallotti P L. Electroless Co-P for diffusion barrier in Pb-free soldering[J]. Electrochim. Acta, 2005, 50(23): 4621-4625.

[16] Chang Y H, Lin C C, Hung M P, Chin T S. The microstructure and magnetic properties of electroless-plated Co-B thin films[J]. J. Electrochem. Soc., 1986, 133(5): 985-988.

[17] Deng B, Wu Y C, Zhang Y, Yang Y, Li G H. Study of electroless plating process for cobalt-boron alloy and its properties(I)[J]. Electroplating & Finishing, 2001, (1): 12-15.

[18] Yang Y, Wu Y C, Qiao Y, Zhang Y, Deng B, Li G H. Study of electroless plating process for cobalt-boron alloy and its properties(II)[J]. Electroplating & Finishing, 2001, (2): 5-7+21.

[19] Shipley C R. Historical highlights of electroless plating [J]. Plat. Surf. Finish., 1984, 71(6): 92-99.

[20] Li N. Practical technology of electroless plating[M]. China: Chemical Industry Press, 2012: 45.

[21] Saito T, Sato E, Matsuoka M, Iwakura C. Electroless deposition of Ni-B, Co-B and Ni-Co-B alloys using dimethylamineborane as a reducing agent[J]. J. Appl. Electrochem., 1998, 28(5): 559-563.

[22] Shacham-Diamand Y, Sverdlov Y, Bogush V, Ofek-Alomg R. A surface adsorption model for electroless cobalt alloy thin films[J]. J. Solid State Electrochem., 2007, 11(7): 929-938.

[23] Stankeviciene I, Jagminiene A, Tamasauskaite-Tamasiunaite L, Sukackiene Z, Gedvilas M, Norkus E. Investigation of electroless deposition of cobalt films by EQCM in the presence of different amines[J]. Mater Sci. Eng. B-Adv. Funct. Solid-State Mater., 2019, 241: 9-12.

[24] Zyulkov I, Armini S, Opsomer K, Detavernier C, De Gendt S. Selective electroless deposition of cobalt using amino-terminated SAMs[J]. J. Mater. Chem. C, 2019, 7(15): 4392-4402.

[25] Chang S Y, Wan C C, Wang Y Y, Shih C H, Tsai M H, Shue S L, Yu C H, Liang M S. Characterization of Pd-free electroless Co-based cap selectively deposited on Cu surface via borane-based reducing agent[J]. Thin Solid Films, 2006, 515(3): 1107-1111.

[26] Cheng S L, Hsu T L, Lee T, Lee S W, Hu J C, Chen L T. Characterization and kinetic investigation of electroless deposition of pure cobalt thin films on silicon substrates [J]. Appl. Surf. Sci., 2013, 264: 732-736.

[27] Yagi S, Kawamori M, Matsubara E. Electrochemical QCM study of the synthesis process of cobalt nanoparticles via electroless deposition[J]. Electrochem. Solid State Lett., 2010, 13(2): E1-E3.

[28] Djokic S S. Electroless deposition of cobalt using hydrazine as a reducing agent[J]. J. Electrochem. Soc., 1997, 144(7): 2358-2363.

[29] Ohno I, Wakabayashi O, Haruyama S. Anodic oxidation of reductants in electroless plating[J]. J. Electrochem. Soc., 1985, 132(10): 2323-2330.

[30] Kim T Y, Lee M H, Byun J, Jeon H, Choe S, Kim J J. Influence of reducing agent on chemical decomposition of bis(3-sulfopropyl) disulfide (SPS) in Cu Plating bath[J]. J. Electrochem. Soc., 2021, 168(3): 032501.

[31] Lee M H, Kim M J, Kim J J. Competitive adsorption between bromide ions and bis(3-Sulfopropyl)-disulfide for Cu microvia filling[J]. Electrochim. Acta, 2021, 370: 137707.

[32] Shingubara S, Wang Z L, Yaegashi O, Obata R, Sakaue H, Takahagi T. Bottom-up fill of copper in high aspect ratio via holes by electroless plating[C]. Shingubara S, Proceedings of IEEE International Electron Devices Meeting, USA: IEEE, 2003.

[33] Shingubara S, Wang Z L, Yaegashi O, Obata R, Sakaue H, Takahagi T. Bottom-up fill of copper in deep submicrometer holes by electroless plating[J]. Electrochem. Solid State Lett., 2004, 7(6): C78-C80.

[34] Wang Z L, Yaegashi O, Sakaue H, Takahagi T, Shingubara S. Bottom-up fill for submicrometer copper via holes of ULSIs by electroless plating[J]. J. Electrochem. Soc., 2004, 151(12): C781-C785.

[35] Wang Z L, Yaegashi O, Sakaue H, Takahagi T, Shingubara S. Suppression of native oxide growth in sputtered TaN films and its application to Cu electroless plating[J]. J. Appl. Phys., 2003, 94(7): 4697-4701.

[36] Lee C H, Lee S C, Kim J J. Bottom-up filling in Cu electroless deposition using bis-(3-sulfopropyl)-disulfide (SPS) [J]. Electrochim. Acta, 2005, 50(16-17): 3563-3568.

[37] Hasegawa M, Yamachika N, Shacham-Diamand Y, Okinaka Y, Osaka T. Evidence for "superfilling" of submicrometer trenches with electroless copper deposit[J]. Appl. Phys. Lett., 2007, 90(10): 101916.

[38] Wang X. Bottom-up filling in electroless plating with an addition of JGB-RPE[J]. Russ. J. Electrochem., 2014, 50 (5): 438-443.

[39] Yang Z F, Li N, Wang X, Wang Z X, Wang Z L. Bottom-up filling in electroless plating with an addition of PEG-PPG triblock copolymers[J]. Electrochem. Solid State Lett., 2010, 13(7): D47-D49.

[40] Wang X, Yang Z F, Wang Z L. Effect of additive triblock copolymer PEP-3100 on bottom-up filling in electroless copper plating[J]. Russ. J. Electrochem., 2012, 48(1): 99-103.

[41] Hasegawa M, Okinaka Y, Shachm-Diamand Y, Osaka T. Void-free trench-filling by electroless copper deposition using the combination of accelerating and inhibiting additives[J]. Electrochem. Solid-State Lett., 2006, 9(8): C138-C140.

[42] Hasegawa M, Yamachika N, Okinaka Y, Shacham-Diamand Y, Osaka T. An electrochemical investigation of additive effect in trench-filling of ULSI interconnects by electroless copper deposition[J]. Electrochemistry, 2007, 75(4): 349-358.

[43] Wang X, Yang Z F, Li N, Liu Z H, Yang Z P, Wang Z L. First synergy effects of SPS and PEG-4000 on the bottom-up filling in electroless copper plating[J]. J. Electrochem. Soc., 2010, 157(10): D546-D549.

[44] Yang Z F, Wang X, Li N, Wang Z X, Wang Z L. Design and achievement of a complete bottom-up electroless copper filling for sub-micrometer trenches[J]. Electrochim. Acta, 2011, 56(9): 3317-3321.

[45] Zan L X, Liu Z H, Yang Z P, Wang Z L. A synergy effect of 2-MBT and PE-3650 on the bottom-up filling in electroless copper plating[J]. Electrochem. Solid-State Lett., 2011, 14(12): D107-D109.

[46] Zan L X, Wang Z L, Liu Z H, Yang Z P. Achievement of bottom-up electroless nickel filling on the SiO_2 surface with Pd-activated SAM[J]. ECS Electrochem. Lett., 2013, 2(1): D1-D3.

化学镀钴和超级化学镀填充的研究进展

沈　钰,李冰冰,马　艺,王增林*

(陕西师范大学化学化工学院, 陕西 西安 710062)

摘要: 随着半导体集成度的不断提高,铜互连线的电阻率迅速提高。当互连线宽度接近 7 nm 时,铜互连线的电阻率与钴接近。IBM 和美国半导体公司(ASE)已经使用金属钴取代铜作为下一代互连线材料。然而,钴种子层的形成和超级电镀钴填充 7 nm 微孔的技术工艺仍是一个很大的挑战。化学镀是在绝缘体表面形成金属种子层的一种非常简单的方法, 通过超级化学镀填充方式, 直径为几纳米的盲孔可以无空洞和无缝隙的方式完全填充。本文综述了化学镀钴的研究进展,并分析了还原剂种类对化学镀钴沉积速率和镀膜质量的影响。同时, 在长期从事超级化学填充研究的基础上, 作者提出了通过超级化学镀钴技术填充 7 nm 以及一下微盲孔的钴互连线工艺。

关键词: 化学镀; 超级化学镀钴; 超级化学镀铜; 铜互连线; 钴互连线